

Zeitschrift: Helvetica Physica Acta
Band: 58 (1985)
Heft: 5

Artikel: Scaling
Autor: Sick, Ingo
DOI: <https://doi.org/10.5169/seals-115626>

Nutzungsbedingungen

Die ETH-Bibliothek ist die Anbieterin der digitalisierten Zeitschriften. Sie besitzt keine Urheberrechte an den Zeitschriften und ist nicht verantwortlich für deren Inhalte. Die Rechte liegen in der Regel bei den Herausgebern beziehungsweise den externen Rechteinhabern. [Siehe Rechtliche Hinweise.](#)

Conditions d'utilisation

L'ETH Library est le fournisseur des revues numérisées. Elle ne détient aucun droit d'auteur sur les revues et n'est pas responsable de leur contenu. En règle générale, les droits sont détenus par les éditeurs ou les détenteurs de droits externes. [Voir Informations légales.](#)

Terms of use

The ETH Library is the provider of the digitised journals. It does not own any copyrights to the journals and is not responsible for their content. The rights usually lie with the publishers or the external rights holders. [See Legal notice.](#)

Download PDF: 01.04.2025

ETH-Bibliothek Zürich, E-Periodica, <https://www.e-periodica.ch>

SCALING*

Ingo Sick

Institut für Physik, Universität Basel, Basel
Switzerland

Scaling phenomena occurring in inclusive scattering from composite systems are reviewed, and examples from nuclear, particle, atomic and solid state physics are discussed. The great usefulness of the observation of scaling for an experimental determination of the reaction mechanism, and the interest in the scaling function for the determination of the target constituent's momentum distribution and form factor, are emphasized.

1. Introduction

Scaling phenomena have played an important role in the development of nuclear- and elementary particle physics. In the late sixties, the discovery of scaling in deep inelastic electron-

* Invited talk presented at the 1985 Spring Meeting of the Schweizerische Physikalische Gesellschaft in Fribourg.

nucleon scattering has provided us with the experimental evidence that nucleons contain massless, pointlike constituents of fractional charge, i.e. quarks. During the last few years, scaling in deep inelastic muon-nucleus scattering has shown evidence that quark momentum distributions in nucleons are influenced by the nuclear medium. The discovery of scaling in inelastic electron-nucleus scattering has allowed us to measure high-momentum components in nuclear wave functions, and it has provided us with an excellent tool to investigate an eventual change of nucleon size due to nuclear binding.

The observation of a scaling behaviour in the inclusive lepton scattering cross section gives us a strong handle on the system under investigation. The fact that scaling is observed yields unambiguous information on the reaction mechanism; such knowledge is a prerequisite for a quantitative exploitation of scattering cross sections. If we do understand the reaction mechanism, the scaling function provides us with an observable that, loosely speaking, represents the momentum distribution of the constituents of the target system. This momentum distribution can be measured in regions of great interest, regions where other attempts have failed.

In this review of scaling phenomena, we want to explain how scaling phenomena come about, and how they can be exploited in different fields of physics. We will mention a number of applications in elementary particle, atomic and solid state physics, before discussing, in somewhat more detail, the most recent developments of scaling approaches, the ones in electron scattering off nuclei.

2. Kinematics

Scaling often is derived during some - not always transparent - theoretical calculation of the scattering cross section.

Here, we want to justify it using the kinematics of the scattering process only. It is the kinematics that is responsible for scaling, and it is this property that makes scaling such a powerful tool.

We will consider the process where a probe (an electron, say) scatters off a system consisting of an initially bound assembly of constituents (say, nucleons in a nucleus). We will be interested in the inclusive scattering cross sections, the one where the scattered probe only is observed. All final states of the rest of the system will be summed over. The kinematical region of interest is the one where the scattering system breaks up and at least one of the constituents is ejected.

For such an inclusive scattering process, the cross section depends on two independent variables \vec{q} and ω . The former one, \vec{q} , is the momentum transferred by the projectile to the scattering system, the latter one, ω , represents the energy transfer. Experimentally, these two variables can be changed at will.

We shall, initially, assume that the impulse approximation (IA) is appropriate for the description of the scattering process, and assume that final state interactions (FSI) of the knocked-out constituent can be neglected. In this case the diagram shown in Fig. 1 describes the reaction. The target constituent before the reaction has momentum \vec{k} and energy E . After the interaction with the projectile the constituent, with momentum $\vec{k} + \vec{q}$, will have a positive energy given by its momentum $((\vec{k} + \vec{q})^2 + m_c^2)^{1/2} - m_c$.

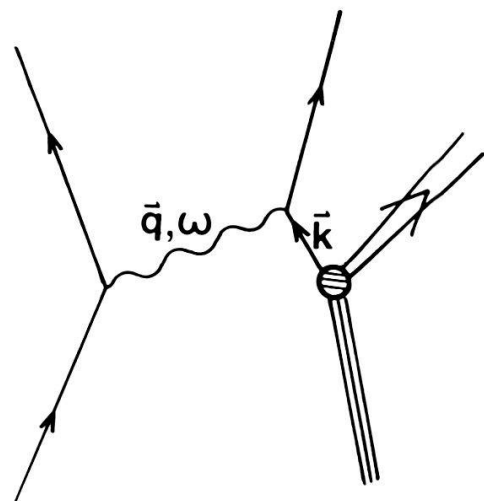


Fig. 1 Impulse approximation diagram for inclusive scattering.

Below we will discuss in more detail the assumption that IA be valid and FSI negligible. Some general considerations, however, can be discussed from the very outset: The projectile interactions with the bound system must be weak, such that multiple interactions of the projectile do not occur. The wave length of the projectile (or, more precisely, of the virtual particle transferring \vec{q} and ω) must be small compared to the distance between the bound constituents; the same should be true for the wave length of the knocked-out constituent C. In this case, the interaction of projectile and constituent may be considered to be localized, and confined to the one constituent of interest. Then we can neglect the interactions of the recoiling constituent on its way through the initially bound target system. Although this interaction may be a strong one, it would not be felt by the projectile, the only particle experimentally observed.

For the process depicted in Fig. 1, energy- and momentum - conservation lead to the following equation

$$\omega = ((\vec{k} + \vec{q})^2 + m_c^2)^{1/2} - m_c + E + E_R \quad (1)$$

The term E_R refers to the recoil energy of the target system minus the knocked-out constituent. Its contribution in general is small, and can be taken into account with the same accuracy as the other terms in eq. (1). Here we will drop E_R , since it complicates the equations without providing additional insight.

In order to better understand the significance of eq. (1), we will split the initial constituent momentum \vec{K} into its components $(k_{\parallel}, k_{\perp})$ parallel and perpendicular to \vec{q} .

$$\omega = ((k_{\parallel} + q)^2 + 2k_{\parallel}q + k_{\perp}^2 + q^2 + m_c^2)^{1/2} - m_c + E. \quad (2)$$

At this point, one makes an important assumption: $q \rightarrow \infty$. Once $k_{\perp} \ll q$, we may neglect the term k_{\perp}^2/q^2 . For $q \rightarrow \infty$, ω also becomes large, so that ω is much larger than the binding energy E of the

constituent. In the limit $q \rightarrow \infty$, eq. (2) simplifies to

$$\omega = (k_{\parallel}^2 + 2k_{\parallel}q + q^2 + m_c^2)^{1/2} - m_c \quad (3)$$

or, schematically

$$k_{\parallel} = z(q, \omega). \quad (4)$$

Equation (4) shows an important finding: the variables \vec{q} , ω are no longer independent. The function z of q and ω , known from kinematics alone, yields k_{\parallel} , the momentum of the constituent before the reaction. In this case, the physics measured by inclusive scattering depends on a single variable $z = z(q, \omega)$. Knowing the cross section along one line in the (q, ω) -plane allows to predict it along any other line by appropriate "scaling".

Under these circumstances the cross section $\sigma(q, \omega)$ will depend on z only; one finds that

$$\frac{d\sigma}{d\Omega d\omega}(q, \omega) / \int \frac{d\sigma}{d\Omega_c}(q) d\omega = F(z) \cdot dz \quad (5)$$

where $\frac{d\sigma}{d\Omega_N}$ is the cross section for elastic scattering of the projectile by the constituent. The sum runs over all constituents of the target system. The function $F(z)$ has an obvious interpretation, the one of the probability to find a constituent with momentum $k_{\parallel} = z$ in the target.

In the following, we will discuss some examples for the use of scaling in different fields of physics. This will allow us to consider in more detail some of the assumptions made, the difficulties that can occur, and the physics results that can be obtained.

3. Deep inelastic electron-nucleon scattering

This first example is the classical one that gave "scaling" its reputation. In the late sixties, a series of experiments carried out at SLAC, with electron beams of energy up to

20 GeV, investigated inelastic scattering from protons. At low excitation energies, the spectra show peaks according to excited states of the proton. At energy loss larger than ~ 1 GeV, a structureless continuum is observed. In this region the cross sections show a then unexpected behaviour. Rather than falling rapidly with increasing momentum transfer, as does e.g. the elastic electron-proton cross section, the inclusive cross sections fall slowly. The ratio $\sigma/\sigma_{\text{Mott}}$, where σ_{Mott} is the cross section for scattering off pointlike objects, is about constant. Moreover, the cross sections are found not to depend on q and ω separately. All cross sections above a certain minimal q , ω depend on the variable $x = (q^2 - \omega^2)/2m_N\omega$ only. Scaling in x is observed.

To illustrate this discovery, Fig. 2 shows the longitudinal and transverse structure functions ¹⁾; measurements at many different values of q, ω define two unique functions depending on x only.

Going back to kinematics (eq. 3) we find that the scaling variable $x=z$ is obtained if m_c is set to zero. ($m_c \neq 0$ yields the y -variable discussed below). This implies that the electron scatters off massless objects. The observation of scaling of $\sigma/\sigma_{\text{Mott}}$ implies that the electron scatters off pointlike objects with elementary cross section proportional to σ_{Mott} . The charge of the constituents turns out to be a frac-

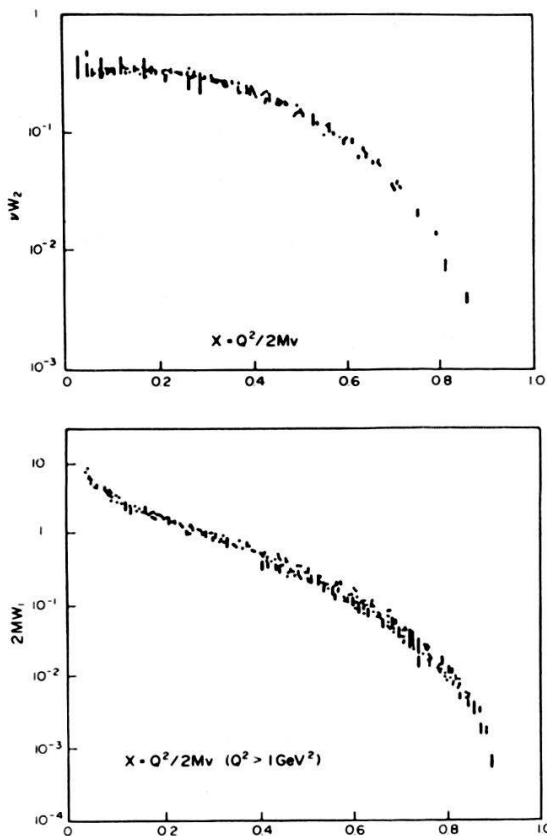


Fig. 2 Structure functions W_1 and νW_2 for electron-proton scattering as function of scaling variable x .

tion of the one of the proton. These observations and its interpretation by J.D. Bjorken and R. Feynman furnished the best evidence for the existence of pointlike, massless constituents, i.e. quarks.

x-scaling in deep inelastic scattering since has been investigated in great detail. Convergence properties due to finite q have been studied, experiments on neutrino inclusive scattering have allowed to separate the contribution of valence - and sea - quarks, etc. x-scaling serves today as the example to demonstrate the power of scaling for the understanding of the reaction mechanism.

The second important feature of scaling, the determination of constituent momentum distributions, actually has not yet fully come to bear. In the infinite momentum frame, the scaling function $F(x)$ represents the probability to find in the nucleon a quark with fraction x of the total momentum of the nucleon. This $F(x)$ at present is hard to understand quantitatively. Quantum Chromo Dynamics (QCD) is a very difficult theory once applied to finite momenta (where data can be measured). Much of the data gathered by experiment, and the wealth of information on scaling properties, will only be understood once QCD theory gets more amenable to practical calculations.

4. Deep inelastic muon-nucleus scattering

During the past few years x-scaling has again produced headlines. An experiment carried out by the EMC group at CERN has studied deep inelastic scattering off nucleons imbedded in nuclei ²⁾. This experiment uses muons of ~ 200 GeV energy produced as a secondary beam at the SPS, and compares the structure function of iron to the one of deuterium (the latter taken as a combination of a free neutron and proton).

This EMC experiment has produced an accurate ratio of the Fe and ²H scaling functions. This ratio, shown in Fig. 3,

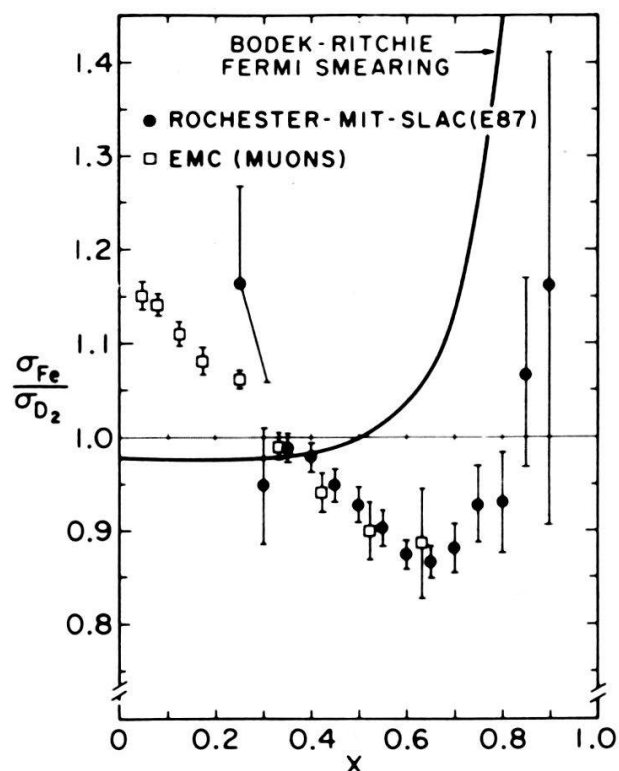


Fig. 3 Ratio of iron and deuterium cross sections as a function of the scaling variable x .

Deviates from one. This result has fascinating consequences for nuclear physics since it shows that the quark momentum distribution in nuclei is influenced by the nuclear medium. Vice versa, it shows that quarks do influence nuclear properties.

Fig. 3 indicates that for $x \leq 0.3$ the iron structure function is larger than the one of the nucleon. This region we do not want to discuss in detail; the experimental situation is not clear given the fact that electron scattering does not yield the same result, and the large number of theoretical interpretations proposed has yet to be sorted out. Deviations from one in this region are to be expected, if we naively connect the low- x sea-quarks to the mesons responsible for the long-range exchange force between nucleons. It seems plausible that number and momentum distribution of these mesons in the medium differ from the ones in the isolated nucleon.

The observation of great interest for nuclear physics is the one that, for $x > 0.3$, the iron structure function is lower than the one for the deuteron. This shows that, in the nuclear medium, it is less probable to find a quark of high momentum (high x). According to the uncertainty principle, this implies a "deconfinement" of quarks, to a volume somewhat bigger than the one in the isolated nucleon. The popular interpretation

for this effect: bound nucleons are "bigger" than free ones.

Over the past few years, a number of authors have advocated an increase of the nucleon size of 20-40% at nuclear matter density. (For a more detailed discussion see below). Such a change of nucleon size clearly would have major consequences for our understanding of nuclei, and the role played by the internal degrees of freedom of the nucleon. In section 7, we will come back to this question. Suffice to say here that this EMC experiment again emphasizes the usefulness of scaling for the measurement of nuclear properties.

5. Electron-atom scattering

The previous two examples dealt with high energy phenomena, i.e. energies of tens of GeV. We now want to briefly illustrate scaling phenomena occurring at much lower energy: the use of scattering of KeV-electrons for the measurement of bound electron momentum distributions in atoms.

When an electron is scattered off an atom, the energy spectrum of the scattered electrons ³⁾ shows the characteristic behaviour displayed in Fig. 4. At low momentum and energy-transfer, the spectrum is dominated by the excitation of discrete atomic shells. At large q , ω the quasielastic peak increasingly dominates. This wide peak results from the scattering off individual, initially bound, electrons in the atom, which are ejected. The quasielastic peak occurs at an energy loss of order $\omega \approx q^2/2m_e$, and has a width and shape that reflects the momentum distribution of the bound electrons.

The inclusive cross section can easily be shown to scale. This scaling behaviour, however, hardly ever is discussed explicitly in atomic physics. The reaction mechanism seems obvious, and needs little experimental verification. The constituents are known, and convergence in terms of increasing q/k quickly achieved. The interpretation of the data in terms of

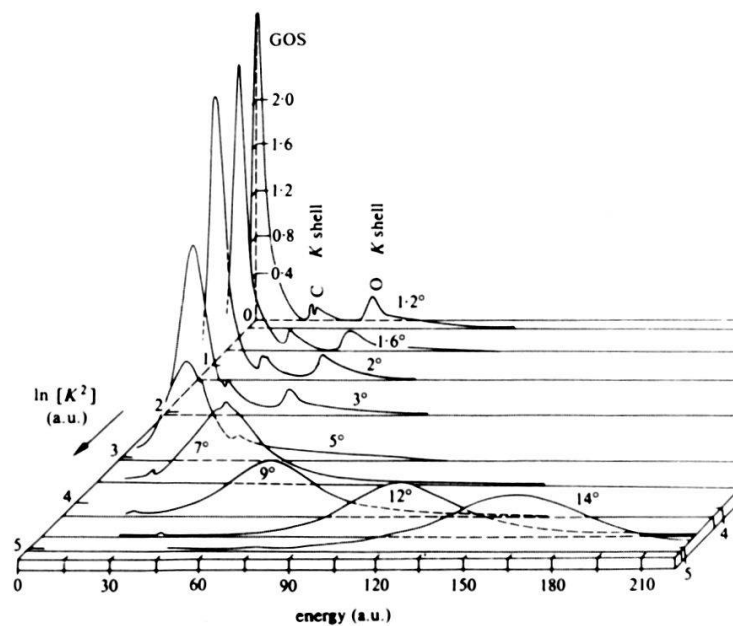


Fig. 4 Bethe surface from electron-CO₂ scattering as a function of momentum transfer (K^2) and energy transfer

momentum distributions therefore is based directly on the Compton-profile, the asymptotic shape of $\sigma(q, \omega)$ converted to the equivalent one observed in Compton scattering. Although scaling is not explicitly mentioned in atomic physics, the physics is the same as the one for γ -scaling discussed below, and analogies are useful for a deeper understanding.

6. Neutron scattering from helium

The examples of scaling given above all deal with leptons as probes. This is comprehensible given the fact that scaling applies only to probes that weakly interact. One-step reactions of the probe are the prerequisite. However, electron scattering is not the only object of interest to scaling studies. Scattering of thermal neutrons, carried out in order to measure momentum distributions of atoms in solid state physics, is another example. The case of neutron scattering is quite similar to

the one of electron-atom scattering. Although the cross sections show the scaling behaviour discussed for high-energy lepton scattering, scaling is rarely discussed explicitly.

Neutron scattering nevertheless is of great interest to the understanding of scaling phenomena in general. In connection with neutron scattering a large effort has gone into the theoretical understanding of final state interaction (FSI) effects. These FSI effects are a worry in inclusive scattering from both nucleons and nuclei, and have not been adequately studied. From neutron scattering we can learn where FSI are important, and where we may ignore them. Studies of FSI effects in neutron scattering have been carried out in particular in connection with scattering from liquid Helium. We therefore will discuss this example in the following.

Superfluid Helium represents an interesting case for the measurement of atomic momentum distributions. Helium atoms are expected, and found to have, the normal momentum distribution due to thermal motion. A small fraction of the superfluid Helium, however, is predicted to have a very different one: the atoms being part of the "Bose condensate" should have, naively stated, zero momentum. Such a Bose condensate thus should lead to a $\delta(k)$ -function of $k=0$ superimposed on the regular k -distribution.

A number of experiments on inclusive neutron scattering have been carried out to detect this Bose condensate. The inclusive cross section $\sigma(q, \omega)$, or equivalently the momentum distribution (i.e. scaling function), does not show the expected result, however. As indicated by Fig. 5, no δ -function is visible near the maximum of the inclusive cross section ($k=0$), even though the experimental resolution was good enough⁴⁾. It is apparent, though, that the peak does not have the standard Gaussian-type shape. A certain pointedness is reminiscent of the δ -function expected.

The "absence" of the δ -function has led to extensive studies⁵⁾ of FSI effects. The Helium atom recoiling in the li-

quid interacts with other atoms according to the atom-atom potential described by the usual Lennard-Jones potential, $r^{-12} - r^{-6}$. This potential is rather strong and singular at small He-He-distances r , and has been bound to indeed influence the inclusive spectrum.

To calculate the effect of FSI, one can write the inelastic response function $s(q, \omega)$ as the imaginary part of the Fourier transform of the Heisenberg density

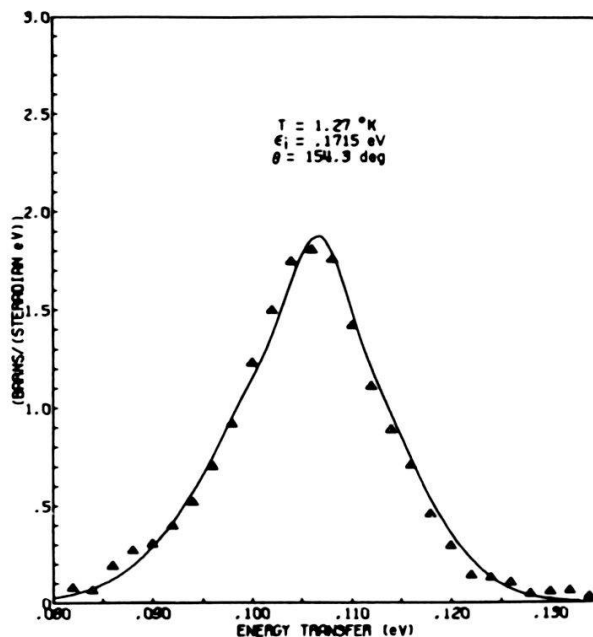


Fig. 5 Cross section for scattering of 0.17 eV neutrons from ${}^4\text{He}$ (1.27°K) as a function of energy loss.

operators $\langle \hat{\rho}(\vec{q}, t) \hat{\rho}(-\vec{q}, 0) \rangle$. Developing the expectation value as a sum of many-body operators yields an expansion containing the first-order FSI effects.

It has been shown that FSI have two distinct effects: The peak of $\sigma(q, \omega)$ (hence $F(y)$) is shifted by an amount given by

$$\Delta\omega \approx 4\pi \frac{\hbar^2}{2m} \cdot \rho \cdot \text{Re}(f(k_R)) \tag{6}$$

Here ρ is the density of the medium the recoil atom interacts with, $f(k_R)$ is the zero-degree Helium-Helium scattering amplitude for recoil momentum k_R . In addition, the peak of $\sigma(q, \omega)$ undergoes a folding, with a width

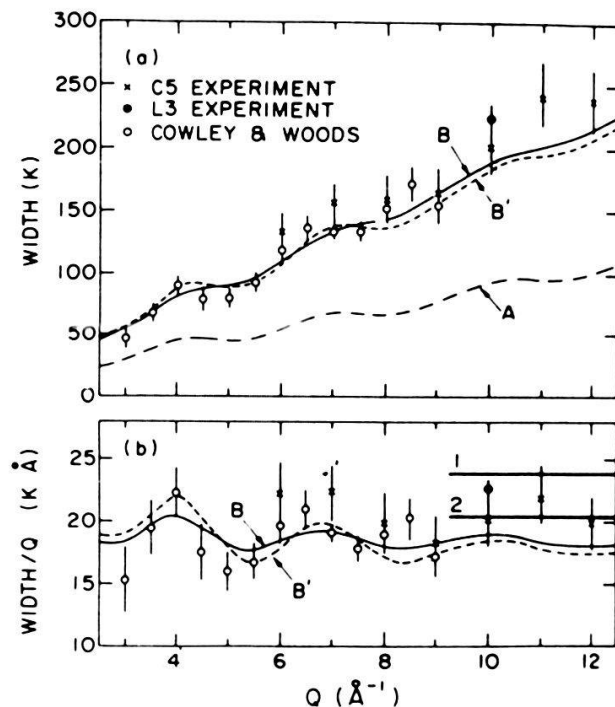
$$\delta\omega = \frac{\hbar}{2m} \cdot k_R \cdot \rho \cdot \sigma_{\text{tot}} \tag{7}$$

where σ_{tot} is the Helium-Helium total cross section. It is this

latter folding that is responsible for the smearing of the $\delta(k=0)$ -function initially searched for in data like the ones of Fig. 5.

For the investigation of FSI effects, neutron-Helium scattering features two nice properties. The FSI is large, so that effects can be observed and compared to theory. In addition, the total He-He cross section is an oscillatory function of the recoil momentum. Accordingly, the smearing width $\delta\omega$ should show the same behaviour, and lead to a small oscillatory change in the width of the quasielastic peak. The experimental width of $\sigma(q,\omega)$ as a function of the recoil momentum is plotted ⁵⁾ in Fig. 6. One observes that the small variation predicted by theory is reproduced. The calculation of FSI effects thus is reasonably well understood. The generalization of FSI effects (eqs. 6,7) to e.g. electron-nucleus scattering is straightforward.

Fig. 6 Width of quasi-elastic peak for n-⁴He scattering as a function of the Helium recoil momentum.



7. Quasielastic electron nucleus scattering

Here we deal with the process where an electron with an energy in the range of several GeV scatters off individual nucleons within the nucleus. These nucleons (but for FSI effects) are ejected from the nucleus. The scaling behaviour of this quasielastic cross section we discuss in detail, since this example deals with the most recent development ⁶⁾ of scaling and the explicit introduction of the y -scaling variable. Moreover, the physics related to y -scaling is particularly rich, and serves to nicely illustrate the diverse ideas.

In quasielastic electron-nucleus scattering we deal with nuclear constituents that have a finite mass m_N . The recoiling nucleons always have momenta large enough to make relativistic kinematics imperative (for non-relativistic energies FSI is too strong to allow for a meaningful application of scaling analysis). According to eq. 3, the appropriate scaling variable then is

$$z = y = (\omega^2 + 2m\omega - q^2)/2q \quad (8)$$

The physical significance of y is (in the limit of large q) the component k_{\parallel} of the nucleon initial momentum parallel to \vec{q} .

The constituents being nucleons, scaling is obtained (eq. 5) if the cross section is divided by the e-N elastic cross section known from electron-nucleon scattering. In order to account for the off-shell nature of the nucleon before scattering, the off-shell cross section ⁷⁾ is used.

The example we want to discuss concerns inclusive scattering on ${}^3\text{He}$, for two reasons. First, this nucleus is singled out by the fact that virtually "exact" Faddeev wave functions for 3 nucleons bound by modern NN-potentials are available; this allows for a significant comparison between experiment and theory. Second, only for ${}^3\text{He}$ do we presently have inclusive data useful for an analysis in terms of scaling; for all heavier nuclei, no

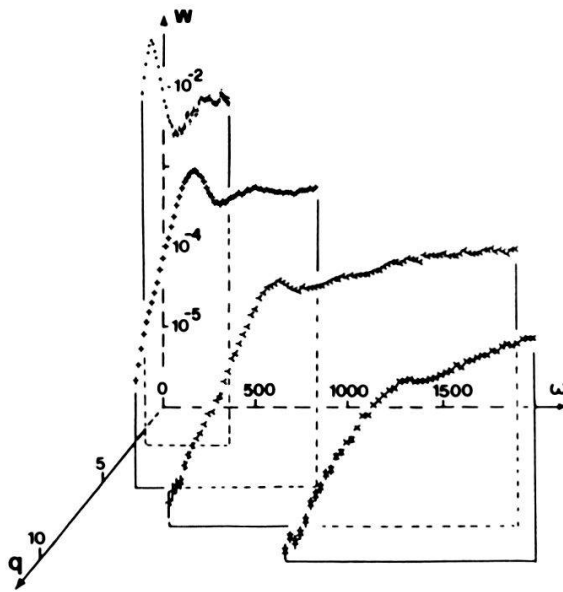


Fig. 7 Inelastic response function for electron- ^3He scattering as a function of energy transfer (MeV) and momentum transfer (fm^{-1}).

data at large q, ω are available.

In Fig. 7 we show a fraction of the ^3He data we measured⁸⁾ at SLAC. At low momentum transfer, the quasielastic peak dominates the cross section. As q increases, this peak widens, shifts to larger energy loss ($\omega \sim q^2/2m_N$), and the continuum of nucleon resonances and deep inelastic scattering gets more and more pronounced. The cross sections of interest for y -scaling, the ones on the low- ω side of the maximum of the quasi-

elastic peak, fall over many decades.

The scaling function computed from these data (plus many other sets covering the low- ω side of the quasielastic peak only) is displayed in Fig. 8. The y -range shown covers the region between low ω (y negative, $x \gg 1$) and the maximum of the quasielastic peak ($y = 0$, $x = 1$). It is immediately apparent from Fig. 8 that an impressive scaling behaviour is observed. Data from many different q, ω define a unique function $F(y)$. The width of the band $F(y)$ is very narrow (and can be understood as a consequence of $q \neq \infty$). While y -scaling previously was a theoretical concept only proposed by West⁹⁾, we have been able to show⁶⁾ with this data that it is realized indeed in nature.

As mentioned above, we can learn two pieces of physics from two distinct observations: the fact that the data do scale, and the numerical value of the scaling function. Let me discuss the latter first.

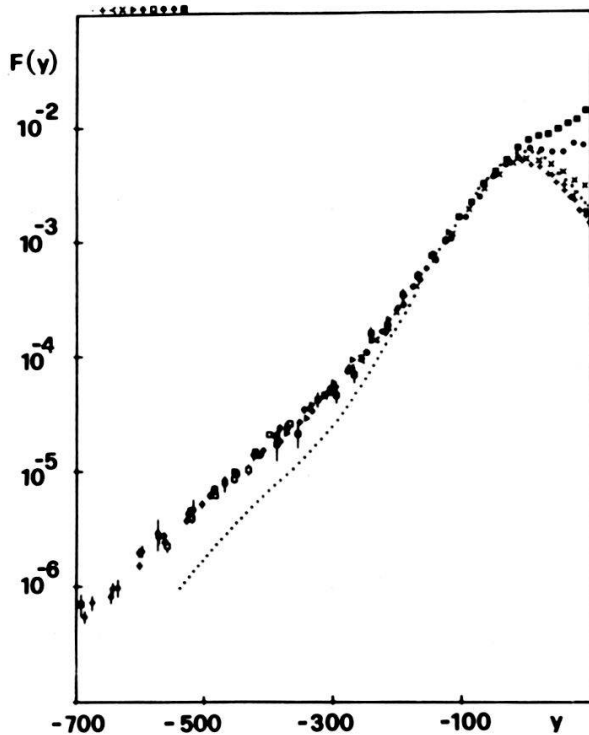


Fig. 8 Scaling function $F(y)$ (c/MeV) as function of y (MeV/c) for ${}^3\text{He}$. The dotted curve represents the Faddeev momentum distribution $\rho(k_{\parallel})$.

is several orders of magnitude lower than the one measured by $(e, e'p)$ at typical $k_{\parallel} \lesssim k_F$. For the first time, the high momentum components become accessible.

In the past, a large effort has gone into attempts to measure components of large k in nuclei, for obvious reasons. Short-range phenomena in nuclei, from two-nucleon correlations to non-nucleonic degrees of freedom, influence the wave function at large momenta. Past efforts to measure these large k have not been successful, basically because in all reactions used a hadronic probe on reaction product was involved¹⁰⁾. The probability to find components of large k is orders of magnitude smaller than the one for low k (Fig. 8). Due to the strong interactions of hadrons, two-step processes involving low k always are more likely than the one-step processes used to search for large k .

The function $F(y)$ represents the longitudinal momentum distribution $\rho(k_{\parallel})$ of nucleons in ${}^3\text{He}$, summed over all nucleons. At first sight, this may not seem to be of particular interest; reactions like $(e, e'p)$ are known to measure momentum distributions in more detail, for individual separation energies (shells). The interest in $\rho(k_{\parallel})$ becomes immediately obvious, though, once one looks at the y -scale of Fig. 8. The maximum value of $y \sim 700$ MeV/c is much larger than the Fermi-momentum k_F . At $k_{\parallel} \sim 700$ MeV/c, the momentum space density

The complexity of the reaction mechanism therefore has kept us from measuring large k .

Inclusive scattering of electrons is not subject to this basic problem. The interaction of electrons is so weak that multistep reactions of the electron are of no concern. The recoiling hadron, which is subject to multistep reactions, is not observed. All final states are summed over. To the extent that q is high enough so that the states of the recoil nucleon form a complete set, FSI of the hadron has no effect on the electron spectrum.

While, a priori, the interpretation of (e, e') should be free of the complexities due to the reaction-mechanism, one would like to have an experimental confirmation. Too often in the past attempts to determine large k have failed because the reaction mechanism was more complicated than anticipated. At this point, the scaling of $d\sigma/d\Omega d\omega$ is vital: it does provide us with the experimental proof that for the selection of data shown in Fig. 8 (the ones for the region of q, ω expected to be free of FSI effects) the reaction mechanism is properly described by impulse approximation! Other reaction mechanisms do not lead to scaling.

To illustrate this point, we give two examples. At energy loss larger than $\omega \sim q^2/2m$, the internal degrees of freedom of the nucleon increasingly influence the inclusive (e, e') spectrum. In particular, the excitation of the Δ_{33} -resonance and Meson Exchange Currents (MEC) start to dominate the cross section. Fig. 9 shows the data ⁸⁾ in this region of q, ω . For $y > 0$, where the Δ -excitation and MEC-processes are important, scaling is not observed. $F(y)$ has a strong dependence on the momentum transfer. The origin of this is obvious. The kinematics for Δ -excitation and MEC processes is not the one for elastic e - N scattering; equation (1) does not apply. In addition, the q -dependence of the form factor for Δ -excitation differs from the one for elastic scattering; equation (5) does not apply either. Figure 9 demon-

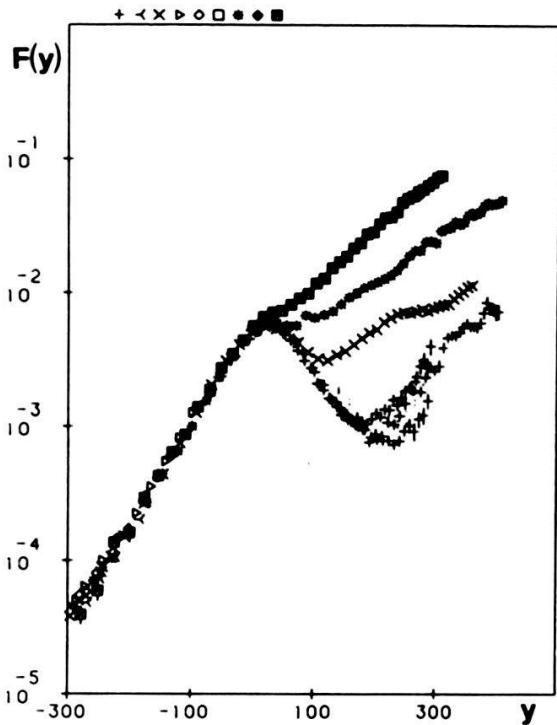


Fig. 9 Scaling function $F(y)$ for ${}^3\text{He}$ and $y > 0$, where Δ -excitation and MEC-processes dominate.

states that scaling is not obtained if the reaction mechanism assumed is not the correct one.

Another property of the reaction mechanism assumed is the one of the unimportance of FSI. At low energy loss, FSI between the knocked-out nucleon and the $(A-1)$ nucleus certainly is important. Calculations ¹¹⁾ of inclusive cross sections indicate that, for $\omega - \omega_{e1} > 100 \text{ MeV}$ FSI are negligible. These calculations cannot be relied upon, however, since they use a cluster model for ${}^3\text{He}$. Direct deuteron knockout is the process postulated to mock up FSI,

while the real process occurring, nucleon knockout with subsequent deuteron formation due to FSI, is not calculated. The effect of FSI can better be estimated using the approach discussed above in the previous section. The folding and shift of the quasielastic cross section, dependent on the NN scattering amplitude and total cross section, is negligible compared to the bin size of the data once the recoil nucleon energy (i.e. $\sim \omega - \omega_{e1}$) is larger than $\sim 100 \text{ MeV}$. Only these data are shown in Fig. 8.

The best test for the (un)importance of FSI is again provided by the scaling property of the data. FSI depend on the relative nucleon- $(A-1)$ nucleus energy in the final state. Due to the energy dependence of this interaction, FSI is large at low ω , small at large ω . For different values of q , and the same y , different regions of $\omega - \omega_{e1}$ contribute. FSI therefore leads to a non-scaling of the data, a feature experimentally observed for

$\omega - \omega_{el} < 100$ MeV. If the data used for the scaling analysis do scale, we have experimental proof that FSI for those data is negligible.

Given the experimental verifications of the reaction mechanism, we may relate $F(y)$ to properties of the initially bound system. Putting aside complications due to non-infinite q (the neglect of k_{\perp} and E) $F(y)$ represents the momentum distribution $\rho(k_{\parallel})$. In Fig. 8 we compare $F(y)$ to the momentum distribution of ${}^3\text{He}$ obtained from a Faddeev calculation¹²⁾. In this calculation, the wave function for 3 nonrelativistic structureless nucleons bound by the Paris nucleon-nucleon interaction is obtained with little approximation. Fig. 8 shows that the calculation underestimates the momentum space density significantly for momenta $k_{\parallel} > 250$ MeV/c ($k \gtrsim 400$ MeV/c). This observation qualitatively agrees with the one made for the elastic $A=3$ charge form factors which, for momentum transfers $q \approx 2k \approx 800$ MeV/c, also are significantly too low.

At present, we have no clear explanation for this difference. We may suspect that the coupling to non-nucleonic degrees of freedom of the ground state wave function is not yet fully treated. While the long-range degrees of freedom, Δ -excitation, are accounted for by modern Faddeev calculations¹²⁾ the shorter-range processes responsible for high k remain to be studied.

Here, we do not want to further discuss this problem; the main emphasis of this article is scaling, not the properties of ${}^3\text{He}$. The important message, carried by the scaling property of the data is the fact that we experimentally can get a handle on the reaction mechanism, the prerequisite for a study of large momenta.

Before leaving the use of $F(y)$ as a momentum distribution, we want to point out that some aspects of y -scaling, the convergence of $F(y)$ with increasing q in particular, merit further study. This convergence actually is quite rapid since in

eq. (3) one neglects terms of order $(k_{\perp}/q)^2$ only (for x-scaling terms of order k_{\perp}/q need to be neglected). For $A=3$ the theoretical wave functions available should allow an in-depth study of the convergence that goes beyond the more phenomenological studies carried out for x-scaling.

In order to account for finite q in the quantitative use of $F(y)$, it is not useful to give up ¹³⁾ the identity of k_{\parallel} and y . This would cause the scaling variable, which must be calculated from experimental observables, to lose its physical meaning. Rather, the value of $F(y)$ can be corrected for the fact that (at $q < \infty$) $F(y)$ represents a projection of $\rho(k_{\perp})$ at a K_{\parallel} which is not strictly constant. Such corrections can be shown to largely compensate deficiencies due to the use of data with finite q .

The last topic concerning y-scaling we want to discuss implicitly again concerns the reaction mechanism. To derive scaling, several properties - in particular the form factor of the constituent in the medium - had to be assumed. If scaling is observed, we can learn something on this form factor.

A number of authors ¹⁴⁾ have considered the possibility that nucleons bound in nuclei differ from free ones. In particular, increases of the nucleon size of 20-40% at nuclear matter density have been suggested. Of these proposals several have been motivated by the data on deep inelastic muon scattering discussed above. Others base their predictions on quark models, or have been inspired by the relativistic $\sigma\omega$ -model.

In order to exploit the occurrence of nucleonic properties in the calculation of the scaling function, it should be noticed that the value of $F(y)$ depends on the nucleon cross section $\frac{d\sigma}{d\Omega_N}$. If nucleons in nuclei differ from free ones, the q -dependence of $\frac{d\sigma}{d\Omega_N}(q)$ will differ as well. Since a given value of y results from different combinations of q and ω , $F(y)$ will not be independent of q unless the proper q -dependence of $\frac{d\sigma}{d\Omega_N}(q)$, the one for the nucleon in the medium, is used.

The scaling property of the data thus yields an ideal test for medium effects on the nucleon form factor¹⁵⁾. One only needs to observe the scaling property of $F(y)$, and does not need to understand the nuclear properties that determine the value of $F(y)$. This situation is analogous to the one discussed above for x -scaling. There the scaling function was calculated assuming pointlike constituents, and the experimental observation of scaling has provided us with the best proof that objects with pointlike form factors do indeed exist.

To determine the bound-nucleon form factor, we again use the (e, e') -data for ${}^3\text{He}$. Only for ${}^3\text{He}$ the region of q (400 - 2000 MeV/c) and ω (100 - 1000 MeV) is sufficiently large to produce a large variation of q (hence $\frac{d\sigma}{d\Omega_N}$) for a given value of y .

In Fig. 8 we have shown the data in terms of the scaling function $F(y)$ calculated using the free nucleon form factors and the off-shell electron-nucleon cross section according to ref.⁷⁾. Fig. 10 again shows the scaling function¹⁵⁾, this time calculated with a parametrization corresponding to a nucleon radius increased by 20%. Obviously, the scaling property is very much degraded, since the width of the band of $F(y)$ is much larger than in Fig. 8. From Fig. 10 we conclude that an increase of about 1/3 of the change made, i.e. $\sim 6\%$, is all that is compatible with y -scaling.

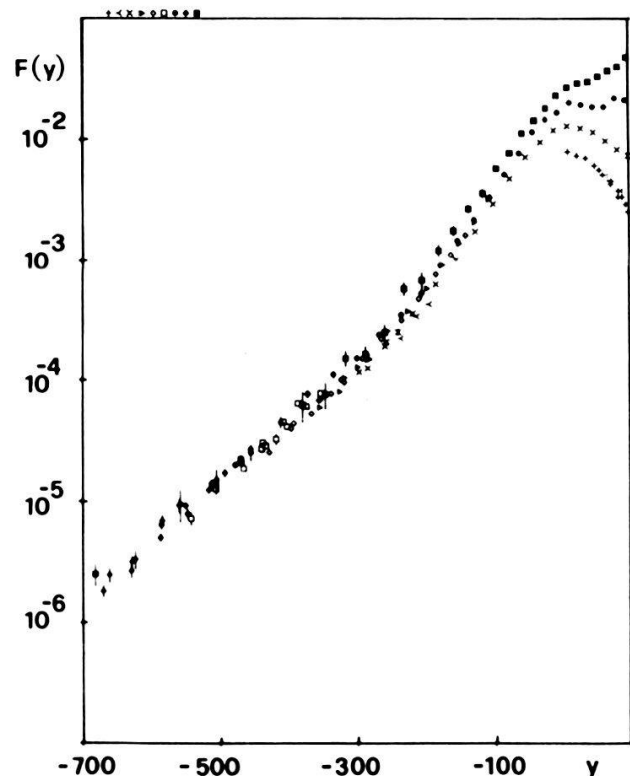


Fig. 10 Scaling function $F(y)$ for ${}^3\text{He}$ calculated assuming a 20% increase of the bound-nucleon size.

Many of the theoretical models used to describe nucleons, like the $\sigma\omega$ - or bag-models, yield a relation of nucleon size R and mass. Basically, these models contain only one scale parameter that fixes both m_N and R . Isolated changes of the nucleon radius thus might not be appropriate. A change of m_N will also influence the scaling property, since $y(q,\omega)$ depends on m_N due to kinematics. We therefore display, in Fig. 11, $F(y)$ for ${}^3\text{He}$ for the case where both R and m_N^{-1} are increased by 10% over their free-nucleon value. When comparing to Fig. 8, we again note a pronounced degradation of the scaling property. One third of the change made, $\sim 3\%$, is all that is compatible with scaling.

Clearly one would like to compare these limits to the radius increase proposed mainly for heavier nuclei ¹⁴⁾. A rough

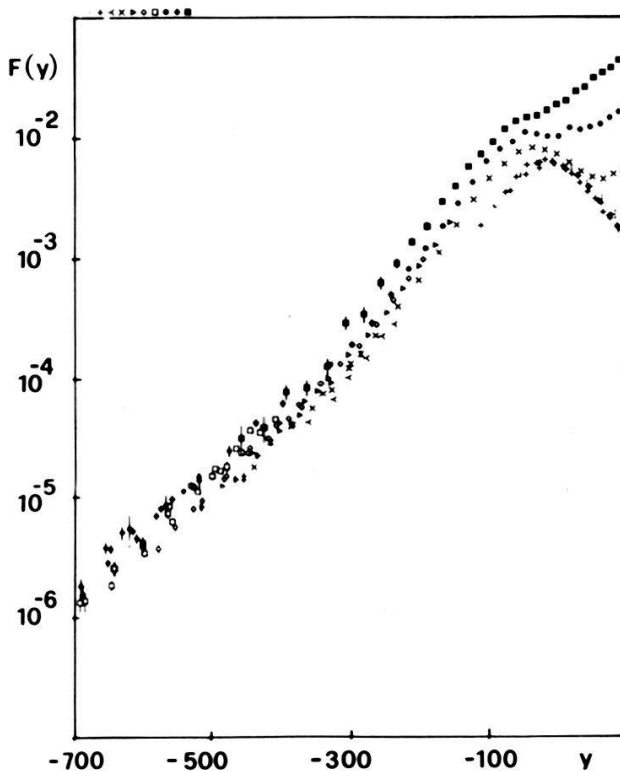


Fig. 11 Scaling function $F(y)$ for ${}^3\text{He}$ calculated assuming a 10% increase of bound-nucleon radius and inverse mass.

comparison can be made without recourse to specific models by realizing that the average nucleon density $\bar{\rho}$ amounts to 50% and 68% of the nuclear matter density $\bar{\rho}_{\text{NM}}$ for ${}^3\text{He}$ and ${}^{56}\text{Fe}$, respectively. While ${}^3\text{He}$ does have a smaller $\bar{\rho}$, medium effects can be expected not to differ drastically from those in ${}^{56}\text{Fe}$, the nucleus discussed above in connection with the EMC effect. The increase of nucleon size we find is much smaller than the ones proposed for heavier nuclei. An experiment we recently carried out at SLAC will measure the radius change of nucleons in heavy nuclei directly.

For systems having as high a density as nuclei, we certainly would expect to find some effect of the nuclear environment on nucleon properties. These effects, however, need not necessarily show up in a change of the average size. A more plausible model might be the one where nucleons get modified only in short-range collisions. The deconfinement of quarks into (say) 6-quark objects of larger size then could be the cause for the decrease of momentum space density at large momenta observed in x-scaling.

8. Conclusion

With this example we want to conclude the discussion of scaling phenomena. Obviously, scaling is not a closed subject. A number of topics like the convergence with q require further study, and data for high energy electron scattering on heavy nuclear targets are eagerly awaited for both x- and y-scaling.

We hope to have shown that scaling phenomena are of great interest in fields as diverse as atomic, nuclear and particle physics. The experimental evidence on the reaction mechanism provided by the scaling property makes the scaling function a highly useful observable for a quantitative study of the target constituent momentum distribution.

9. References

- 1) A. Bodek, Phys. Rev. D20 (1979) 1471
- 2) J.J. Aubert et al., Phys. Lett. 105B (1981) 322
- 3) P. Martel et al., Journ. Low Temp. Phys. 23 (1976) 285
- 4) A.L. Bennani et al., Chem. Phys. Lett. 41 (1976) 470
- 5) L.J. Rodriguez, H.A. Gersch, H.A. Mook, Phys. Rev. A9 (1974) 2085

- 6) I. Sick, D. Day, J.S. McCarthy, Phys. Rev. Lett. 45 (1980) 871
- 7) A.E.L. Dieperink, T. de Forest, I. Sick, R.A. Brandenburg, Phys. Lett. 63B (1976) 261
- 8) D. Day et al., Phys. Rev. Lett. 43 (1979) 1143
- 9) G. West, Phys. Rep. C18 (1975) 264
- 10) I. Sick, Proc. Workshop Prog.Options Int. Energy Phys., Los Alamos, 1979, LA-8335-C
- 11) J.M. Laget, Phys. Lett. 151B (1985) 325
- 12) C. Hajduk, P.U. Sauer, W. Strueve, Nucl. Phys. A405 (1983) 581 and priv. com.
- 13) C. Ciofi degli Atti, E. Pace, G. Salme, Phys. Lett. 127B (1983) 303
- 14) J.V. Noble, Phys. Rev. Lett. 46 (1981) 412
F.E. Close, R.G. Roberts, G.G. Ross, Phys. Lett. 129B (1983) 346
L.S. Celenza, A. Rosenthal, C.M. Shakin, Phys. Rev. Lett. 53 (1984) 892
I.T. Cheon, S.J. Choi, M.T. Jeong, Phys. Lett. 144B (1984) 312
- 15) I. Sick, Nucl. Phys. A434 (1985) 677